Autonomic Neuroscience: Basic and Clinical 164 (2011) 51–61

Contents lists available at ScienceDirect

Autonomic Neuroscience: Basic and Clinical

journal homepage: www.elsevier.com/locate/autneu

Neuronal loss and abnormal BMP/Smad signaling in the myenteric plexus of diabetic rats

Stella M. Honoré [a], Laura C. Zelarayan [b], Susana B. Genta [a], Sara S. Sánchez [a,*]

[a] Dpto. Biología del Desarrollo, INSIBIO (Consejo Nacional de Investigaciones Científicas y Técnicas-Universidad Nacional de Tucumán (CONICET-UNT)), Chacabuco 461, T4000ILI San Miguel de Tucumán, Argentina
[b] Max Delbruck Center for Molecular Medicine, Berlin, Germany

ARTICLE INFO

Article history:
Received 6 November 2010
Received in revised form 8 June 2011
Accepted 9 June 2011

Keywords:
Diabetes
Small intestine
BMP/Smad signaling
Enteric nervous system

ABSTRACT

Bone morphogenetic proteins (BMPs) are critical molecules during gut morphogenesis. However, little is known about their participation in the homeostasis of adult gut and their possible role in diseases. Gastrointestinal complications occur during diabetes with loss of enteric neurons. In this study, we investigated the possible involvement of BMPs signaling pathway in diabetic enteric neuropathy in an experimental model of diabetes in rats. The expression of BMPs, BMPs receptors and intracellular Smad effectors were assessed in control and diabetic smooth muscle layer of jejunum by immunofluorescence, Western blot and RT-PCR methods. Myenteric neurons and glial cells were measured by immunofluorescence using specific markers. In addition, cell apoptosis was evaluated by means of direct and indirect techniques. We demonstrated that diabetic ganglia displayed a significant decrease in ganglion size due to enhanced apoptosis and loss of peripherin. A decrease in glial fibrillary acidic protein (GFAP protein) was also observed in enteric glial cells. BMP-2 was down-regulated in the myenteric plexus of diabetic rats at 3 and 9 weeks. A loss of enteric neurons by apoptosis was correlated with an ectopic BMP-4, increased BMPR-Ia and nuclear p-Smad1 expression in the myenteric plexus. Insulin-treatment prevented the intestinal alterations observed. These findings suggest that diabetes is associated with an abnormal BMP/Smad signaling expression in the myenteric ganglia that affects the homeostasis of the enteric plexus.

1. Introduction

Diabetes mellitus is the most common multisystemic endocrine disorder. Longterm, poorly-controlled diabetes mellitus often results in gastrointestinal complications (Horowitz et al., 1991; Spångéus et al., 1999). Frequent vomiting, diarrhea, constipation, fecal incontinence, abdominal pain and unpredictable changes in blood glucose are major clinical problems in diabetic patients (Koch, 1999; Ricci et al., 2000; Bytzer et al., 2001; Rayner and Horowitz, 2006). These gastrointestinal afflictions are not normally life-threatening but profoundly affect the quality of life. In many cases, these symptoms are thought to be due to abnormal gastrointestinal motility that, in turn, may be a manifestation of degenerative changes in the peripheral nervous system (Tougas et al., 1992; Kniel et al., 1996). In diabetic autonomic neuropathy was evidenced by vagal nerve dysfunction, sympathetic nerve damage, and alterations in the enteric neurons (Camilleri and Malagelada, 1984; Tougas et al., 1992; Watkins et al., 2000; He, 2001; Yoneda et al., 2001; Furlan et al., 2002).

The enteric nervous system (ENS) is an integrative network composed of neurons and enteric glial cells located along the wall of the gastrointestinal tract (Jabbur et al., 1988; Rühl et al., 2004; Rühl, 2005). Enteric neurons respond to luminal contents and smooth muscle tension. Thus, the ENS coordinates the intricate peristaltic movements, initiating local reflexes to regulate motility and secretion (Bywater et al., 1987).

A reduction in the number of myenteric neurons and alteration in their size have been noted in several gastrointestinal segments of diabetic animal models, including streptozotocin-induced (STZ-induced) diabetic rodents (Hernandes et al., 2000; Büttow et al., 1997; Furlan et al., 2002; Fregonesi et al., 2001; Chandrasekharan and Srinivasan, 2007). However, the way in which diabetes affects enteric neurons is not well understood yet.

Bone morphogenetic proteins (BMP) comprise a subgroup of the TGF-β family of secreted signaling molecules. BMP-2 and 4 transduce their signal by binding to a heterodimer consisting of a type I receptor (BMPR-IA or BMPRIB) and a type II (BMPR-II) receptor (Nohe et al., 2002). Receptor activation leads to phosphorylation and activation of the Smad signaling cascade (Shi and Massagué, 2003; Zwijsen et al., 2003; Feng and Derynck, 2005). BMPs regulate multiple critical functions during organogenesis, including specification, regionalization and differentiation within the developing gut (Grunz, 1996; de

* Corresponding author. Tel.: +49 54 381 4107214; fax: +49 54 381 4247752x7004.
E-mail address: ssanchez@fbqf.unt.edu.ar (S.S. Sánchez).

1566-0702/$ – see front matter © 2011 Elsevier B.V. All rights reserved.
doi:10.1016/j.autneu.2011.06.003

Santa Barbara et al., 2005; Batts et al., 2006; Rubin, 2007). BMP-2 and BMP-4 have been implicated in the normal development of the enteric nervous system in animals and humans (Brewer et al., 2005; Chalazonitis et al., 2004; Goldstein et al., 2005). Even though BMPs are involved in gut embryogenesis, their role in the adult organ has not been fully studied yet, nor has their participation in diabetes been investigated so far.

In this study, we looked for evidence of BMPs signaling in the myenteric plexus of the small intestine and examined the effects of hyperglycemia on BMP/Smad activation in an experimental rat model of diabetes. We hoped to provide further data concerning damage to enteric neurons in diabetic rat and its underlying mechanism.

2. Materials and methods

2.1. Animals and experimental design

Male Wistar rats weighing ~200–250 g were obtained from the animal facility of the INSIBIO (Instituto Superior de Investigaciones Biológicas, San Miguel de Tucumán, Argentina). All animals were housed at constant temperature (22 °C) under a 12:12-h light–dark cycle, with free access to water and a standard laboratory chow. The following experiments were conducted in agreement with the Guide for the Care and Use of Laboratory Animals (Institute of Laboratory Animal Resources, Commission on Life Sciences, National Research Council, National Academy Press, Washington, DC), and the local Institutional Animal Care Committee. Animals were randomly divided into four groups of fifteen animals each: diabetic for 3 weeks (D3w); diabetic for 9 weeks (D9w), insulin-treated diabetic for 3 weeks (D + Ins) and normal control. Briefly, diabetes mellitus was induced by a single intraperitoneal injection of freshly prepared streptozotocin (50 mg/kg body weight) in citrate buffer (0.1 M, pH 4.5) (Sigma, St Louis, Mo, USA), as described previously (Sánchez et al., 2000). Control rats received an equal volume of citric acid buffer alone. Animals showing fasting glucose levels higher than 350 mg/dl 3 days after STZ treatment were included in the study as diabetic animals. Once the diabetic state was established, animals in the D + Ins group were subcutaneously injected with a daily insulin dose of 3.4–4.5 IU/g body weight (Betasint, Laboratorios BETA) to restore normoglycaemia. This treatment was carried out twice a day for 3 weeks whereas the effects of diabetes are evident even at this early.The groups of animals (D3w; D9w, D + Ins and control) were pair-fed with standard rat chow and had free access to water. Glucose levels and weight were recorded every week during the experimental period and at the time of euthanasia.

2.2. Tissue sampling

Fasted rats were deprived of food for 24 h and killed by cervical dislocation at 3 and 9 weeks after diabetes induction. The abdomen was opened along the midline and small intestine was dissected from rats. The first ten centimeters closest to the stomach were removed. From this point three pieces of proximal jejunum (5 cm) were cut along the mesentery and pinned down flat onto a glass dish with Sylgard silicone coating. The segments of jejunum were rinsed with ice-cold phosphate-buffered saline (PBS; pH 7.4) and immersed in Bouin's fixative overnight at 4 °C for classical histology and immunohistochemical assays.

2.3. Immunofluorescent labeling

Three-micrometer sections were dried overnight at 37 °C and then deparaffinized and rehydrated. The slides were immersed in 10 mM citrate buffer (pH 6.0) and treated with microwave irradiation to unmask binding epitopes prior to antibody staining. The slides were then left to stand for 10 min in buffer at room temperature before thorough washing in tap water. After three washes in PBS the slides were incubated with 2% bovine seroalbumin (BSA) for 30 min at room temperature. Then they were incubated overnight at 4 °C with the primary antibodies diluted in PBS with 10% normal serum (specific antibodies and dilutions used are listed in Table 1). For double-labeled sections, primary antibodies were mixed and incubated as a cocktail. After three washes in PBS, incubation with the secondary Alexa Fluor 488 or Alexa Fluor 594 (Invitrogen) antibody was performed (1 h, at room temperature). The sections were then washed five times in PBS and mounted in aqueous mounting medium with antifading agents (Biomeda, Foster, CA). All secondary antibodies were confirmed to be species-specific for their individual primary antibody. Negative control included omission of the primary antibody and mismached secondary antibody. The staining was not observed in the negative controls. Aditionally p-Samd1 antibody was pre-incubated with the respective blocking p-Samd1 peptide (sc-12353 P, Santa Cruz biotech.) (10^{-6} or 10^{-5} M in blocking buffer) raised against peptide antigen overnight at room temperature, prior to incubation with tissue/sample. Tissue sections probed with neutralized antibodies were compared with tissue sections probed with antibody alone (no blocking peptide). Staining recognized by the respective antibodies was absent in the tissue probed with neutralized antibody. Double-immunolabeled sections were examined by laser scanning confocal microscopy with an Olympus FV300 instrument equipped with an multi-line Argon laser (457 nm, 488 nm, 515 nm), Ar laser (488 nm), HeNe-Green laser (543 nm) and HeNe-Red laser (633 nm).

The number and distribution of myenteric neurons and glial cells were determined in cross sections by analysis of adjacent microscope fields throughout the length of the jejunum pieces. This represented at least 40 non-adjacent microscope fields (approximately 8.5 mm) in each tissue. To detect changes in the content of neurons in the ganglia, the average number of Toluidine blue and peripherin-positive cells appearing within the myenteric ganglia was determined in these sections. The study was performed in a blinded manner in non-adjacent stained sections obtained at 50 μm intervals using an Olympus BX80 fluorescence microscope.

The intensity of the ganglia stained for specific glial marker GFAP and BMPR-Ia was measured in non-adjacent cross sections of the jejunum, using the ImageJ 1.44 software (NIH Image). At least 35 non-adjacent microscope fields were analyzed in each tissue. Data included average intensity, standard deviation of the intensity, integrated intensity, maximum and minimum greyscale levels and

Table 1
Antibodies used.

	Host	Dilution[a]	Catalog no.	Source
Primary antibody				
Peripherin	Rabbit	1:100	sc-28539	Santa Cruz Biotech
Peripherin	Mouse	1:100	sc-58833	Santa Cruz Biotech
GFAP	Rabbit	1:100	G9269	Sigma
S-100B	Mouse	1:100	MAB079-1	Chemicon
Active caspase 3	Rabbit	1:100	G3781	Promega
BMP2	Goat	1:50	sc-6895	Santa Cruz Biotech
BMP4	Mouse	1:20		Dr. K. Masuhara (Osaka, JP)
BMPRIa	Goat	1:50	sc-5676	Santa Cruz Biotech
Smad1	Mouse	1:50	sc-7965	Santa Cruz Biotech
p-Smad1	Goat	1:100	sc-12353	Santa Cruz Biotech
β-actin	Mouse	1:250	A5316	Sigma
Secondary antibody				
Alexa Fluor 488 anti-goat IgG	Rabbit	1:2000	A11078	Invitrogen
Alexa Fluor 488 anti-mouse IgG	Goat	1:1500	A11001	Invitrogen
Alexa Fluor 594 anti-rabbitt IgG	Goat	1:2000	A21207	Invitrogen
Alexa Fluor 594 anti-mouse IgG	Goat	1:2000	A11005	Invitrogen

[a] Dilution used in immunohistochemical and immunofluorescence studies.

threshold area (expressed as a percent of total stained ganglion area). The nuclei of myenteric cells stained for p-Smad1 were outlined using a draw tool in the software and the intensity was measured. About 200 p-Smad-positive nuclei per group were assessed in each experiment.

2.4. Determination of apoptosis

Apoptotic cells were identified using terminal deoxynucleotidyl transferase dUTP nick end labeling (TUNEL) method. The TUNEL assay was performed according to manufacturer's instructions (DeadEnd™ Fluorometric TUNEL System no. G3250; Promega). Briefly, deparaffinized slides were fixed in 4% paraformaldehyde and treated with proteinase K to permeabilize the tissues. The slides were incubated with a labeling reaction mix using rhodamine or fluorescein as fluorophore for 1 h at 37 °C. The reaction was stopped by the addition of 2x saline-sodium citrate (SSC) buffer and 3 washes in PBS were made before tissue was mounted in a fluorescence mounting medium (DAKO Corp., CA, USA). TUNEL labeled sections were incubated with a solution containing anti-peripherin and anti-GFAP (rabbit polyclonal) anti-S100B (mouse monoclonal) primary antibodies. Alexa 488 and Alexa 594 antibodies (Invitrogen) were also applied and the slices were mounted. Apoptotic cells were also identified on activated caspase-3 stained sections to avoid the nonspecific staining with TUNEL. Staining for activated caspase-3 was performed using a rabbit polyclonal antibody (Promega) (Table 1). Sections were rinsed with PBS and blocked with 2% BSA in PBS (1 h, room temperature) and then double labeled for peripherin (mouse monoclonal). Alexa 488 goat anti-rabbit and Alexa 594 anti-mouse are used as secondary antibodies. Assessment of TUNEL$^+$ and activated caspase-3$^+$ cells in preparations from was performed in a blinded manner. About 500 peripherin-positive cells were assessed in each experiment for colocalization with either TUNEL or activated caspase-3 immunoreactivity in adjacent sections. To avoid duplicate counting of the same cells counting was performed non adjacent sections obtained at 50 μm intervals.

2.5. Electrophoresis and immunoblot analysis

The mucosa and submucosa were peeled away under a dissecting microscope and the muscle layers (circular and longitudinal) with the myenteric plexuses were rinsed twice with PBS. The muscle layers obtained were homogenized in lysis buffer composed of 50 mM Tris–HCl pH 7.4, 0.1 M NaCl, 1% Nonidet P-40, 2 mM PMSF, a Complete Protease Inhibitor Cocktail (Roche), and then sonicated (three times, 10 s each, midpower) on ice. Protein concentration was determined by Lowry's method (Lowry et al., 1951). The samples were boiled for 4 min in 2% SDS, 2% 2-mercaptoethanol, 20 mM Tris–HCl, pH 7, and placed (50 μg of protein/lane) on 7.5% SDS-polyacrylamide gel. After electrophoresis, the proteins were transferred to a nitrocellulose membrane (Hybond-C super; Amersham, Buckinghamshire, UK). Protein detection was performed by immunoblot analysis using specific anti-monoclonal and polyclonal antibodies as shown in Table 1. The detection of the ligands, receptors and Smad antibody-complexes was performed using a biotin-extrAvidin-peroxidase system (Sigma). Peroxidase activity was detected incubating blots in 3,3-diaminobenzidine-H_2O_2. Beta actin was used as an internal standard. The relative intensity of the obtained products was measured using the ImageJ 1.44 software (NIH Image).

2.6. Mesurement of BMPs and BMPR mRNA in the jejunum

Real-time reverse transcription polymerase chain reaction (RT-PCR) was performed to detect the expression of BMPs and BMPR mRNAs. Total RNA was purified from the intestinal muscle layers using illustra RNAspin Mini Isolation Kit (GE, Germany) as described by the manufacturer. cDNA was synthesized using AMV-RT (Amersham) and oligo-dT primer (Genbiotech S.R.L.). The expression of related genes was quantified using the SYBR Green Analysis (Qiagen) on an iCycler instrument (Bio-Rad) as described previously (Baurand et al., 2007). PCR was performed in optimized conditions: 95 °C denatured for 10 s followed by 30 cycles of 5 s at 95 °C, 5 s at 58 °C and 35 s at 72 °C and one cycle of 15 s at 95 °C. Specific PCR primers were designed from rat sequences available in the databanks: BMP-2 (NM_017178.1: forward primer 5′-AGCCAAACACAAACAGCGGAAG-3′ and reverse primer 5′-GGAGTTCAGGTGATCAGCCAGG-3′), BMP-4 (NM_012827.1: forward primer 5′-GGATGCTGCTGAGGTTAAAGAAG-3′ and reverse primer 5′-TGGGGAGGAGGAGGAAGAAGAG-3′) and β-actin (NM_031144.2: forward primer 5′-CACACCCGCCACCAGTTC-3′ and reverse primer 5′-CCCATACCCACCATCACACC-3′). Each experiment was performed three times. No other products were amplified because melting curves showed only one peak in each primer pair. A standard curve was created by sequential dilution of the amplified fragment in order to calculate the RNA copy number. Fluorescence signals were measured over 30 PCR cycles. mRNA levels for BMPs were standardized against β-actin mRNA levels in the same mRNA. The mean value for the control animals was set at 100%.

2.7. Statistical methods

Data are presented as means ± SEM. Significant differences between groups were tested by analysis of variance (ANOVA) and Student's t test and a p value of <0.05 was considered statistically significant.

3. Results

3.1. Animal study

Table 2 lists the characteristics of the animals studied. Diabetes resulted in a significant increase in blood and urine glucose and a decrease in body weight in D3w and D9w rats compared to the age-matched controls ($p<0.05$). Total length and weight of the D3w and D9w intestines were significantly increased compared to control. The hypertrophy index, measured as the ratio of small intestine weight to body weight as described previously (Zador et al., 1993; Sánchez et al., 2000), increased in D3w and Dw9 rats ($p<0.05$). Insulin treatment of diabetic rats kept clinical and biochemical parameters at control level (Table 2).

In control jejunum the myenteric ganglia were organized in networks of nerve fibers and cell bodies spread uniformly between the inner and outer muscle layers. Ganglia were packed with clearly visible neurons stained with peripherin (Fig. 1A). In contrast, D3w and D9w showed fewer neurons and obvious gaps in the myenteric

Table 2
Physiological features of animals in study.

Parameters	Control	D3w	D9w	D + Ins
Blood glucose (mg/dl)	117.9 ± 24.5	467.9 ± 23.1[a]	572.6 ± 19.3[a]	140.3 ± 11.5[b,c]
Urine glucose	negative	positive	positive	negative
Body weight (g)	299.4 ± 12.8	202.4 ± 32.5[a]	197.9 ± 31.4[a]	265.3 ± 22.5[b,c]
Intestinal weight (g)	6.9 ± 0.9	11.1 ± 1.2[a]	12.4 ± 0.7[a]	7.7 ± 0.4[b,c]
Intestinal/body weight (%)	2.3 ± 0.5	4.9 ± 0.9[a]	5.8 ± 0.9[a]	2.7 ± 0.2[b,c]
Intestinal length (cm)	90.09 ± 3.5	103.6 ± 4.7[a]	105.5 ± 6.2[a]	88.2 ± 4.1[b,c]

Values represent means ± SEM (n = 15 in each group).
[a] ($p<0.05$) compared to controls.
[b] ($p<0.05$) compared to D3w.
[c] ($p<0.05$) compared to D9w.

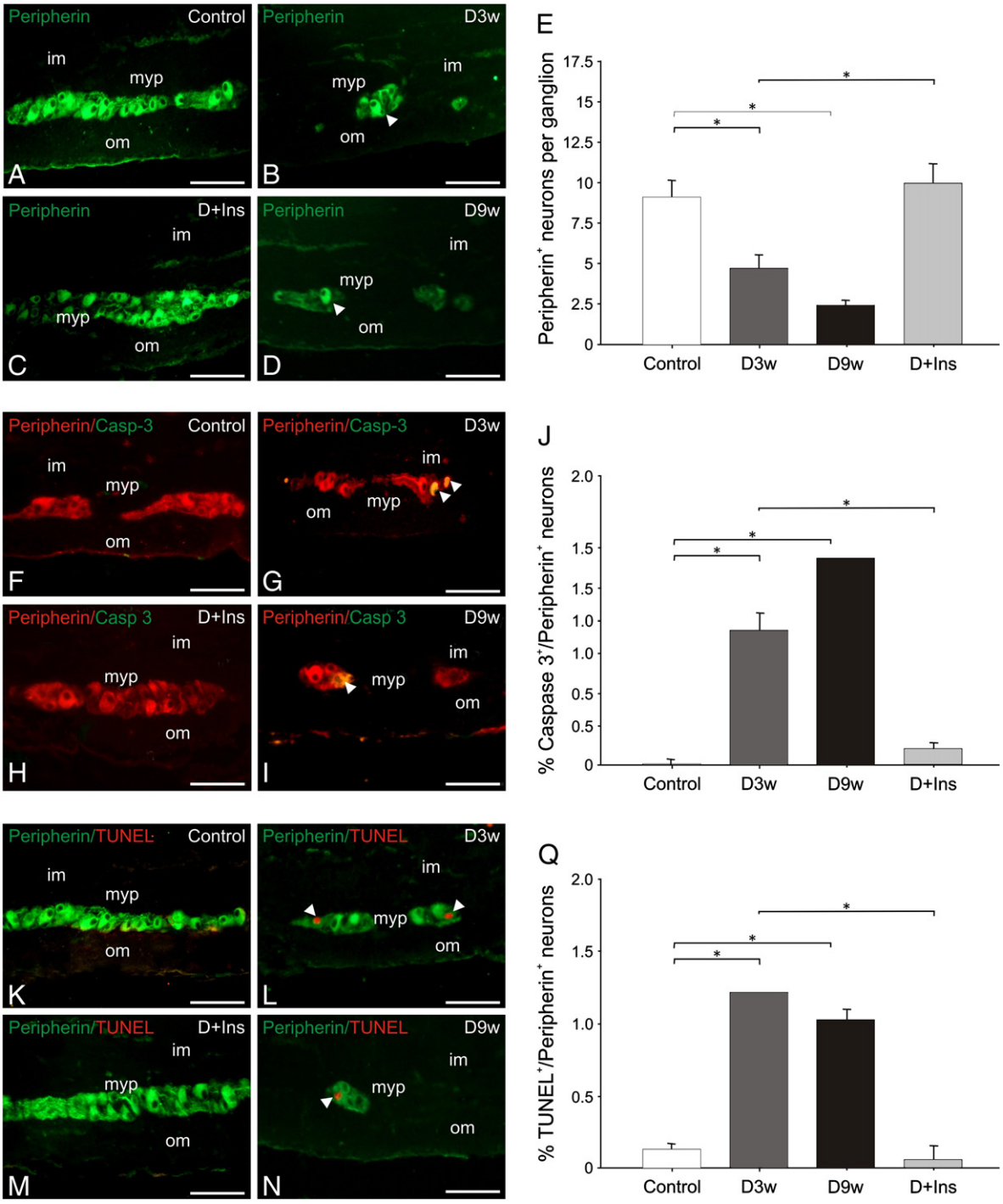

Fig. 1. Micrographs showing the immunodetection of the neuron marker peripherin in cross sections of the muscle layer of control (A), D3w (B), D9w (C), D + Ins (D) intestines. Diabetes causes a strong diminution in enteric neurons (B, D, arrowhead) which is prevented by insulin treatment. Number of peripherin-stained neurons per ganglion in each group (E). A total of 3 independent experiments was performed. Data are represented as mean ± SEM. $^*p<0.05$; $n=10$ per experimental group. Double-labeling immunohistochemistry for cleaved caspase-3 (green) and peripherin (red) in control (F), D3w (G), D9w (H), D + Ins (I) are shown. Apoptosis in the D3w, D9w ganglion is identified by yellow staining due to colocalization of cleaved caspase-3 and peripherin (G, H, arrowhead). The number of activated caspase 3-positive neurons per ganglion in different groups compared with control (J). A total of 3 experiments was performed. Data are represented as mean ± SEM. $^*p<0.05$; $n=10$ per group. Representative sections of the muscle layer of control (K), D3w (L), D9w (M), D + Ins (N) jejunum assessed by TUNEL (red) and peripherin (green) immunostaining. Note that diabetes induces apoptosis of enteric neurons (L, M, arrowhead). Number of TUNEL-positive enteric neurons per ganglia in different groups compared with control (J). A total of 3 experiments was performed. Data are represented as mean ± SEM. $^*p<0.05$; $n=10$ per group. im: inner muscle layer; myp: myenteric plexus; om: outer muscle layer. Bars: A-D, F-I, K-N: 50 μm.

ganglia were observed (Fig. 1B, D arrowhead). Assessment of peripherin revealed that D3w jejunum had a significant decrease in neurons content compared to control gut ($p<0.05$) (Fig. 1E). A more significant neuron reduction was observed in the D9w compared with controls and D3w rats ($p<0.05$) (Fig. 1E). Some sections were stained with toluidine blue to test if "gaps" in ganglia may have been due to loss of neuronal peripherin staining rather than neuronal loss. No staining was observed within these profiles (data not shown)

confirming that peripherin staining was a reliable indicator of neuronal loss. The decrease in neuron number was correlated with the presence of activated caspase-3$^+$/peripherin$^+$ within the myenteric ganglia of D3w and Dw9 animals (Fig.1G, H arrowhead). The number of activated caspase-3$^+$ neurons per ganglion in the different groups is shown in Fig. 1J. D3w and Dw9 animals had a significantly higher number of TUNEL$^+$ neurons in the myenteric ganglia compared to control rats ($p<0.05$) (Fig. 1O). Since damage to enteric neurons was evident as early as 3 weeks of diabetes, the preventive insulin treatment was carried out up to this time. Fig. 1C, H and M show the effects of insulin-treatment in 3 weeks diabetic intestine. The increase in apoptosis observed in D3w ganglia was ameliorated in the D + Ins group ($p<0.05$) (Fig. 1J, O). Total numbers of peripherin$^+$ neurons were similar to control ones ($p>0.05$) (Fig. 1E).

When analyzing the number of enteroglial cells in the jejunum, no significant differences were found between groups (data not shown). However we observed a strong reduction in the intensity of GFAP staining in D3w intestines compared to control ones (Fig. 2A, B). In D9w rats a greater reduction of GFAP staining was observed in the gut (Fig. 2D). Insulin treatment prevented the phenotypic alterations of the glia in the D3w jejunum (Fig. 2C). This qualitative impression was confirmed by the densitometric analysis (Fig. 2E) ($p<0.05$).

3.2. Smads in the diabetic intestine

We next determined whether morphological changes seen in the diabetes state were associated with an altered BMP/Smad signaling. As phosphorylation and nuclear translocation of BMP receptor-activated p-Smads are the hallmarks of ongoing BMP signaling (Rosendahl et al., 2002), the occurrence of nonphosphorylated and phosphorylated Smad1 was analyzed by Western blotting (Fig. 3A). An significative decrease (1.3-fold) ($p<0.05$) in Smad1 protein level was observed in D3w intestines. No significant changes were found in the protein Smad1 content among control and D9w gut ($p>0.5$) (Fig. 3B). However, p-Smad1 protein level increased markedly in D3w (3.5-fold) and D9w (2-fold) compared to control and D + Ins guts ($p<0.05$) (Fig. 3C). The p-Smad1/Smad1 ratio evidenced an important up-regulation of the BMP pathway in the muscle layer in both Dw3 (4.4-fold) and D9w (2-fold) intestines ($p<0.05$) (Fig. 3D).

Immunolocalization of p-Smad1 in control and D + Ins animals showed several intensity degrees of nuclear p-Smad1 staining ranging from weak to moderate in myenteric plexus cells (Fig. 4A-F arrowhead). A weak staining in the nucleus of muscle cells was also observed (Fig. 4A-F, arrow). Diabetes resulted in an increased staining of nuclear (arrowhead) and cytoplasmic (asterisk) p-Smad1 in most ganglion cells of myenteric plexus (Fig. 4G-L). Besides, both the inner and outer muscle layer of the intestines of the Dw3 and D9w rats evidenced intense nuclear p-Smad1 immunoreactivity (Fig. 4G-L, arrow). Intensity levels p-Smad1 in the nuclei of the myenteric cells are shown in Fig. 4M.

3.3. BMP receptor expression in the diabetic intestine

To determine the potential role of BMP receptors in activating Smad 1, we analyzed the expression patterns of BMPR-Ia by Western blotting (Fig. 5A). The analysis revealed a moderate up-regulation of BMPR-Ia protein in the intestines of D3w (3.4-fold) and in D9w (1.9-fold) compared to control values ($p<0.05$) (Fig. 5B). Insulin-treatment maintains BMPR-Ia protein level similar to control value (Fig. 5B). The intensity of BMPR-Ia immunostaining was higher in the myenteric ganglia of D3w rats than in those of control ones (137.5 ± 2.1 arbitrary units vs. 43.2 ± 5; $p<0.05$) (Fig. 5C, I). The immunostaining of D9w intestines (data not shown) revealed lower BMPR-Ia intensity (68.3 ± 7.1 arbitrary units) than D3w intestines ($p<0.05$). Insulin treatment reduced the BMPR-Ia immunostaining intensity observed in D3w rats (58.5 ± 8 arbitrary units) (Fig. 5I). Double inmmunostaining assay for BMPR-Ia (Fig. 5C, F, I arrowhead) and peripherin (Fig. 5D, G, J) revealed that neural cell population is responsible for BMPR-Ia expression in the myenteric plexus (Fig. 5E, H, K arrowhead).

3.4. BMP expression in the diabetic intestine

In order to determine the potential ligands responsible for the induced BMP activity observed in diabetic small intestine, we compared the expression levels of BMP ligands at the RNA and protein levels. As shown in Fig. 6A, BMP-2 mRNA levels in the jejunum of Dw3 rats were significantly decreased (1.4-fold) ($p<0.05$). This reduction response was more evident in D9w rats (5-fold) ($p<0.05$). BMP-4 mRNA levels were strongly increased (2-fold) in D3w intestines ($p<0.05$). However, BMP-4 mRNA increased less (1.5-fold) in D9w rats (Fig. 6B). D + Ins rats showed BMP-2 and BMP-4 mRNA expression similar to control rats ($p<0.05$).

BMP protein bands determined by Western blot analysis are shown in Fig. 7A. Diabetes resulted in a significant down-regulation of BMP-2 protein levels in the jejunum. At 3 and 9 weeks of diabetes, BMP-2 decreased 2-fold and 3.5-fold respectively ($p<0.05$) (Fig. 7B). A different result was found for BMP-4. There was a significant

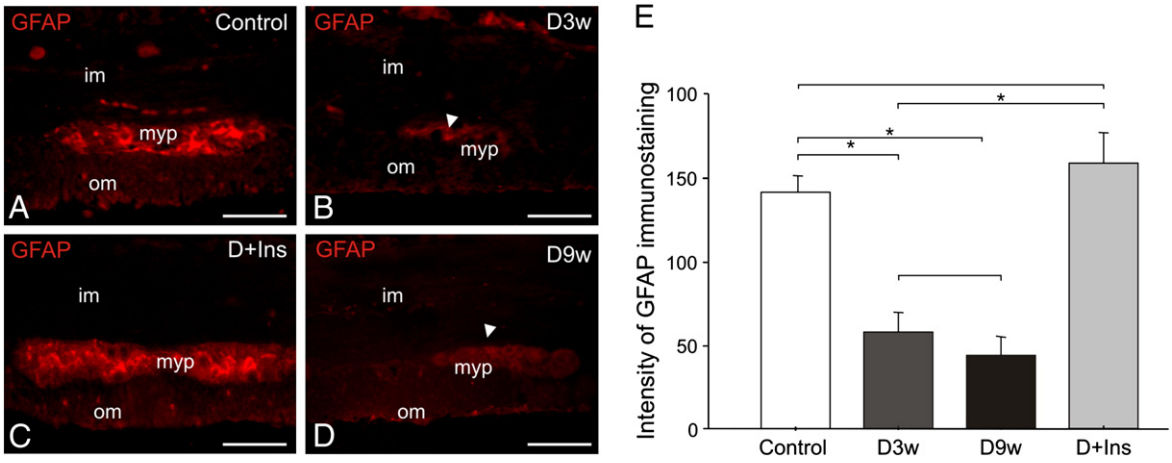

Fig. 2. Micrographs showing the immunodetection of the glial marker GFAP in cross sections of the muscle layer of control (A), D3w (B), D9w (C), D + Ins (D) animals. A clear decrease in reactivity for GFAP in the plexus of D3w and D9w, diabetic animals can be observed (B, C, arrowhead). Mean levels of GFAP-immunoreactive intensity in all the groups. A total of 3 independent experiments was performed. Data are represented as mean ± SEM. *$p<0.05$; $n=10$ per group. im: inner muscle layer; myp: myenteric plexus; om: outer muscle layer. Bars: A-D: 50 μm.

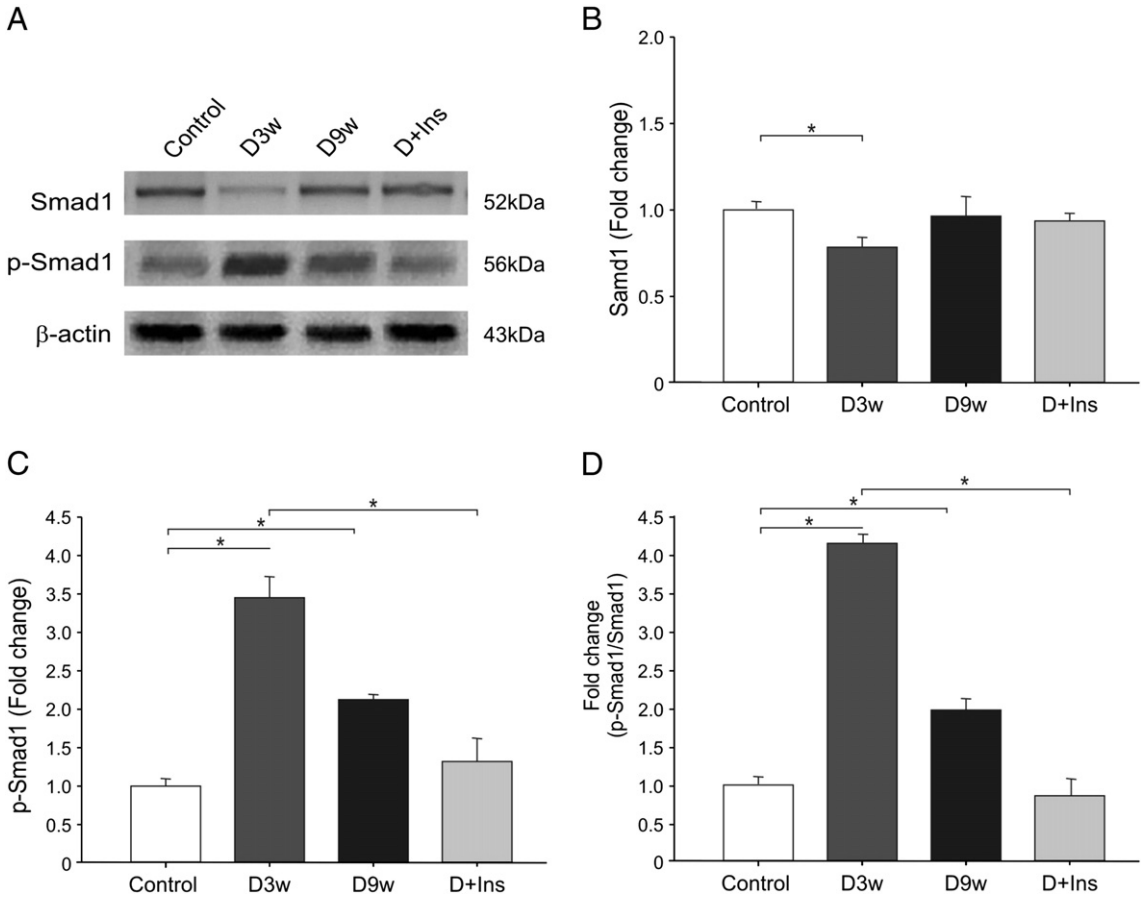

Fig. 3. Representative Western blot of p-Smad1 and total Smad1 assessed in the jejunum muscle layer of control, D3w, D9w, D + Ins rats (A). Relative mean protein levels of Smad1 (B) and p-Smad1 (C). Fold change of p-Smad1 to Smad1 in the jejunum muscle layer of control, D3w, D9w, D + Ins rats assessed by Western blot analysis (D). A total of 3 independent experiments was performed. Data are normalized to control results for each experiment and are represented as mean ± SEM (C, D). *$p<0.05$; $n=8$ animals per group.

induction of BMP-4 protein in D3w (1.6-fold) and D9w (1.2-fold) intestines (Fig. 7C). Insulin treatment maintains the BMP-2 and BMP-4 protein levels similar to control ($p<0.05$).

We also determined the cellular localization of BMP-2 and BMP-4 ligands in control and diabetic smooth muscle layer using indirect immunofluorescence techniques. BMP-2 was found in the cytoplasm of some myenteric plexus cells and in the smooth muscle cells of the outer muscle layer (asterisks) in control (Fig. 7) and D + Ins rats (Fig. 6s). In contrast, the inspection of jejunum sections of D3w and Dw9 animals revealed an overt decrease in immunostaining for BMP-2 (Fig. 6E). No staining for BMP-4 was observed in the myenteric plexus region or in the muscle layer of control and D + Ins jejunum (Fig. 6F). Interestingly, a positive immunoreactivity for this molecule was noted in the myenteric plexus region of D3w animals (Fig. 6G, arrowhead). No staining in the myenteric cells was found in D9w. Weak BMP-4 staining at the outer muscle layer was also found in D3w and in Dw9 intestine.

4. Disscussion

Diabetes is associated with several changes in motor and sensory gastrointestinal functions that have important consequences in the morbidity and effective management of diabetic patients (Goyal and Spiro, 1971; Bytzer et al., 2001; Rayner et al., 2001; Rayner and Horowitz, 2006). Several studies in human biopsies and experimental models have indicated that diabetes causes damage to the enteric nervous system (Watkins et al., 2000; He, 2001; Yoneda et al., 2001; Furlan et al., 2002; Liu et al., 2010).

Using an in vivo STZ-induced diabetic model, we demonstrated a decrease in the number of myenteric neurons 3 weeks after the onset of diabetes, followed by a further neuronal loss at 9 weeks of evolution. Previous studies reported loss of enteric neurons in the stomach, duodenum, caecum and colon of rats with streptozotocin-induced diabetes at more advanced stages of the disease (Büttow et al., 1997; Fregonesi et al., 2001; Furlan et al., 2002). Such differences could be explained by the fact that diabetes has a differential effect on the various intestinal regions of the rats, the distal segments being affected last (Fregonesi et al., 2001).

TUNEL-positive cells were identified only in the myenteric plexus of diabetic gut indicating apoptotic cell death as a possible mechanism of enteric neuronal loss in diabetes. Apoptosis, oxidative stress, advanced glycation end products and their receptors, and changes in nerve growth factors have been proposed as main mechanisms involved in diabetic neuropathy (Schmeichel et al., 2003; Anitha et al., 2006; Chandrasekharan and Srinivasan, 2007). Activated caspase-3 assessment in the intestine of D3w rats confirmed that neurons are comitted to cell death at early stages of the disease and predicted the neuronal loss observed in D9w animals. Moreover, the apoptotic cells observed in D9w gut suggest that neuron number will continue to decrease, probably resulting in a worsening of symptoms over time. In agreement with this idea, He (2001) and Chandrasekharan et al. (2011) determined that a reduction in specific types of neurons in jejunum and colon was implicated in motility disturbances in long-term diabetes patients.

It was suggested that the reduction in the number of myenteric neurons leads to hyperplastic and hypertrophic changes in the intestinal walls during diabetes (Nakabou et al., 1974). This fact,

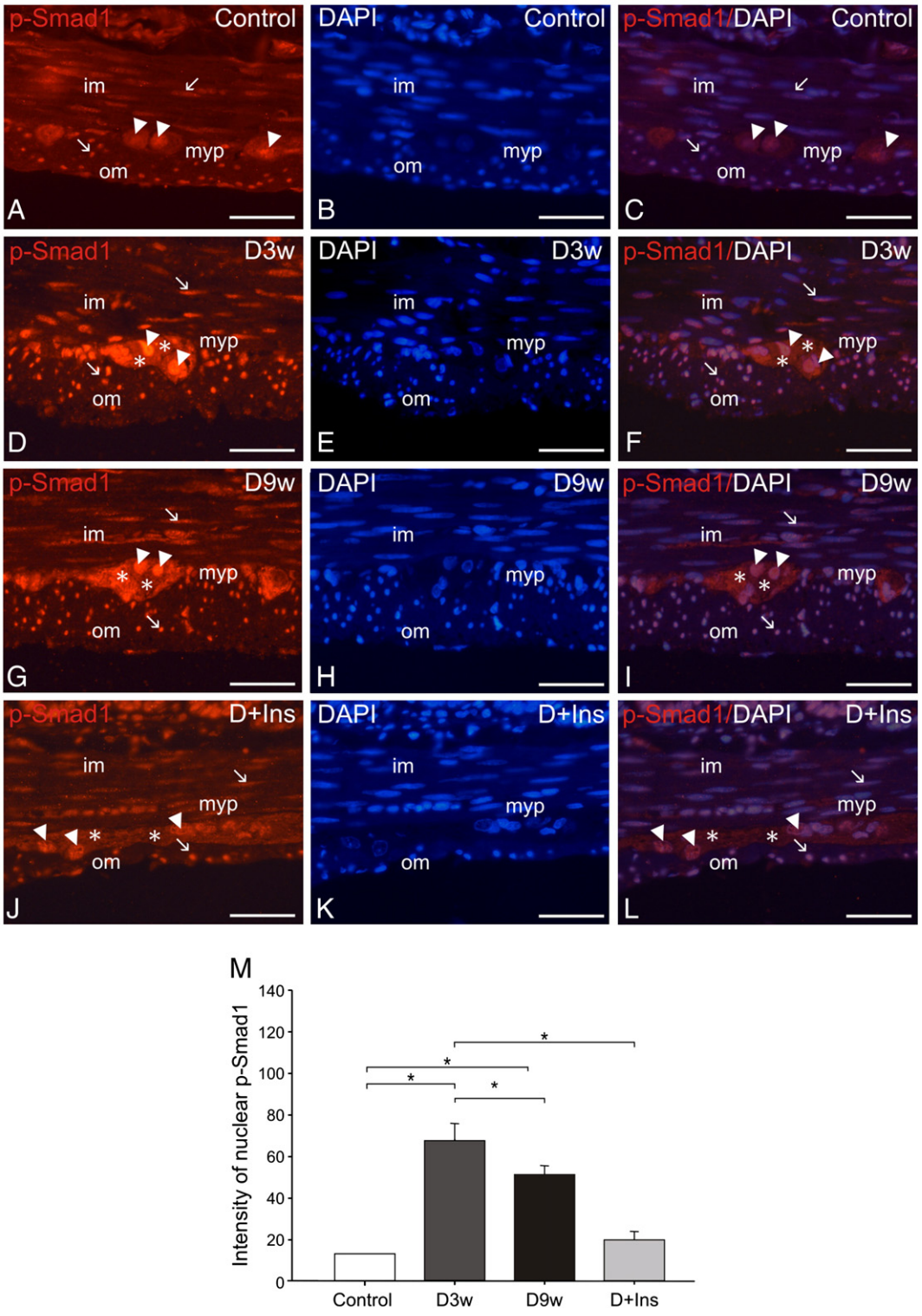

Fig. 4. Representative photomicrographs showing the immunohistochemical detection of nuclear p-Smad1 in the intestinal muscle layer of control (A, C), D3w (D, F), D9w, (G, I), D + Ins (J, L) rats. DAPI nuclear staining of the same sections (B, E, H, K). Note the increased staining for p-Smad1 in the nuclei (arrowhead) and cytoplasm (asterisk) myenteric plexus cells of D3w (D, F), D9w, (G, I) compared to control stain (A, C). Smooth muscle cells of control (A, C) D3w (D, F), D9w, (G, I) rats also presented nuclear p-Smad1 (arrows). A total of 3 independent experiments was performed. $n = 15$ per group. Mean levels of p-Smad1 intensity in myenteric nuclei of different groups studied. A total of 3 independent experiments was performed. Data are represented as mean ± SEM. $^{*}p < 0.05$; $n = 10$ per group. Im: inner muscle layer; om: outer muscle layer; myp: myenteric plexus. Bars: A-L: 50 μm.

together with the reported extracellular matrix accumulation (Sánchez et al., 2000), could also explain the increased intestinal weight/body weight ratio found in the diabetic animals.

On the other hand, we observed that diabetes-induced caspase-3 activation could be prevented by insulin treatment. This effect on neuron homeostasis could be the result of insulin action on both glucose and intermediary metabolism with overall anabolic effects (Biolo et al., 2008). The literature has shown that insulin also has an important function in the modulation of the cellular processes in different tissues, including the nervous tissue (Caldeira and Cagnon,

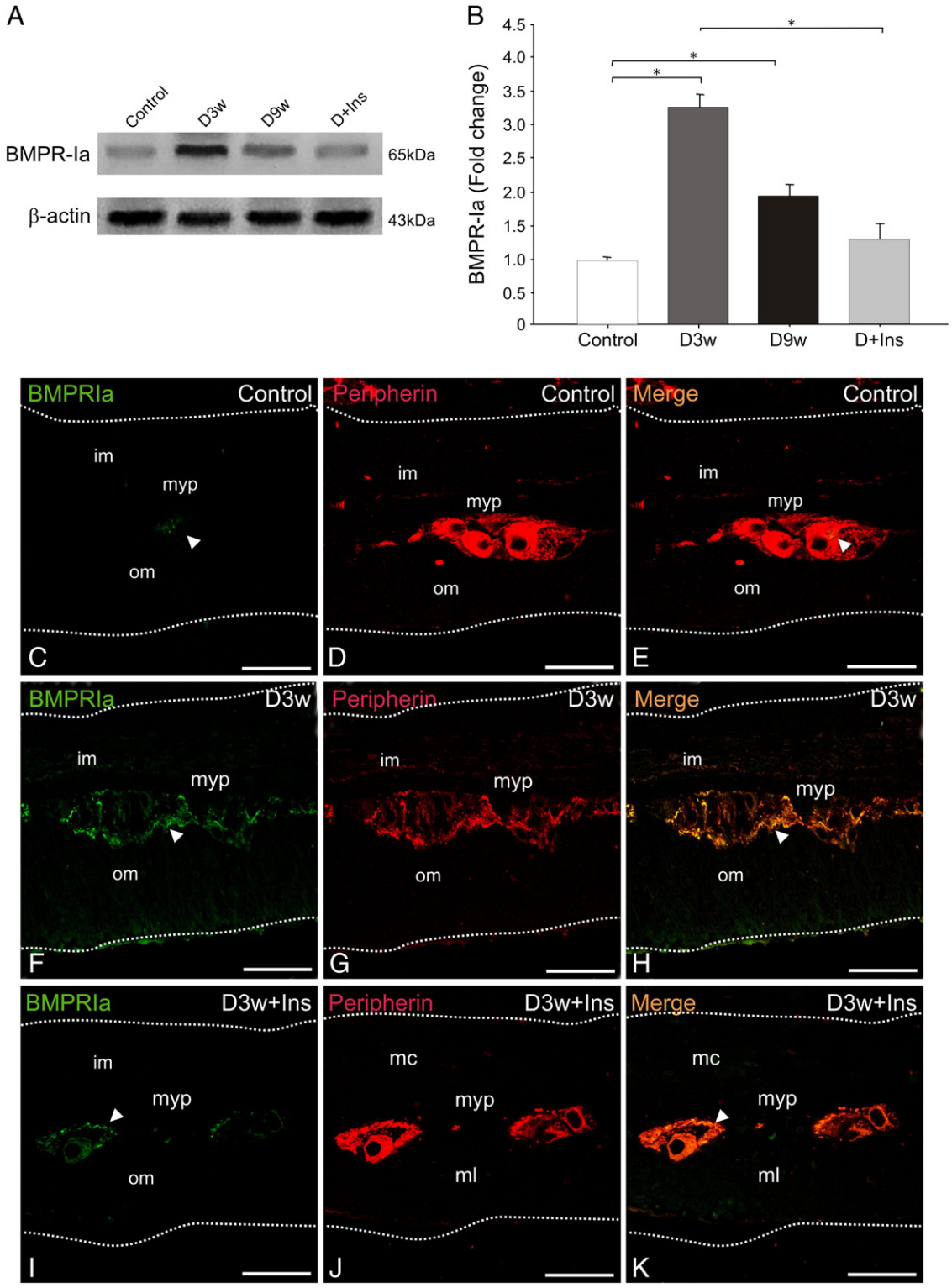

Fig. 5. Relative mean protein levels of BMPR-Ia in the jejunum muscle layer of control, D3w, D9w, D + Ins rats are shown in representative Western blot bands (A). A total of 3 independent experiments was performed. Data are normalized to control results for each experiment and are represented as mean ± SEM; $^{*}p<0.05$; $n = 10$ per group (B). Immunodetection of BMPR-Ia in cross sections of the muscle layer of the intestine of control (C), D3w (F) and D + Ins (I) animals. Note the increased expression of this receptor in the myenteric plexus of diabetic animals (F, arrowhead). Insulin treatment prevented the diabetics changes in BMPR-Ia expression pattern (I). Arrows point to the myenteric ganglion stained with peripherin (red) in the same sections (D, G, J). Yellow staining represents BMPR-Ia expression due to colocalization with peripherin (E, H and K). A total of 3 independent experiments was performed; $n = 12$ in each group. im: inner muscle layer; myp: myenteric plexus; om: outer muscle layer. Bars: C-K: 50 μm.

2008). Wang et al. (1992) and Huang et al. (2003) demonstrated that insulin promotes neuron survival, prompts neurons to synthesize neurofilament axon lattice proteins, and reverses diabetes-induced changes in neuronal mitochondrial function.

We also demonstrated that diabetes leads to a significant decrease in GFAP immunoreactive density in D3w intestines which becomes more notorious in D9w rats. In keeping with our results, Liu et al. (2010) found a similar alteration in myenteric glial cells of diabetic colon, suggesting

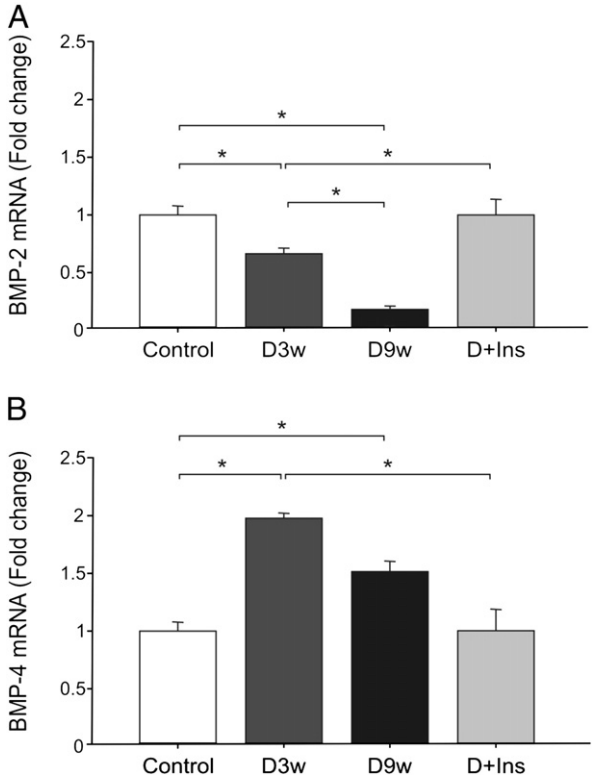

Fig. 6. Real-time reverse transcription polymerase chain reaction showed transcript expression of BMP-2 (A) and BMP-4 (B). Note a decreased expression of BMP-2 and the increase in BMP-4 in D3w and D9w intestines compared to control and D + Ins. Data are represented as mean ± SEM. $^{*}p<0.05$; $n=10$ per group.

that unviable extracellular conditions such as hyperosmolarity, low nutrient availability, increased oxidative stress or the lack of insulin could be involved in phenotypic changes of enteric glial cells. In fact, we demonstrated that insulin treatment preserves the control phenotype of the enteric glia. It has been suggested that insulin plays an important role in astrocyte differentiation and function, regulating GFAP expression in vitro (Aizenman and de Vellis, 1987; Toran-Allerand et al., 1991). So, it is possible that decreased insulin in poorly controlled diabetic animals might contribute to the alterations in GFAP expression in diabetes. In agreement with the above, Coleman et al. (2010) recently demonstrated that insulin treatment prevents diabetes-induced alterations in GFAP content in rats with 4 and 8 weeks of diabetes. These data confirm that the glial cells of the enteric system are also affected by diabetes.

It has been suggested that the decrease in neurotrophic factors could be involved in the pathobiology of diabetes (Anitha et al., 2006). Besides, a reduction in neurotrophins expression was observed in the colon of diabetic rats related to phenotypic glial change (Liu et al., 2010). Neurotrophic factors have been shown to play an important role in the survival and maintenance of peripheral somatic and autonomic neurons (Unger et al., 1998; Lee et al., 2001; Lee et al., 2002; Liu et al., 2010). In our model, we found neuron and enteroglial alterations, and these findings raise the interesting possibility that an impaired glial–neuron interaction takes place in the diabetic jejunum with an abnormal neurotrophin production.

In the present paper we investigate the expression of other paracrine factors belonging to the BMPs family in the muscle layer of rat small intestine during early diabetes. We demonstrated, for the first time as far as we know, that BMPs and the associated Smad signaling are present in the muscle layer, particularly in the myenteric plexus cells of the normal and diabetic adult gut. Active BMP-mediated signaling in the tissues was monitored by the phosphorylation and nuclear location of Smad1. We found that almost all myenteric and smooth muscle cells presented p-Smad1 nuclear staining in the control adult gut, demonstrating that these cells respond to BMP signaling. This fact led us to think that the BMP signaling pathway could play an active role in neuron, glial and smooth muscle cells homeostasis during adulthood as has been shown during enteric development (Chalazonitis et al., 2004).

Interestingly, diabetes increased p-Smad1 levels in the muscle layer, showing a stronger nuclear p-Smad1 staining within ganglion cells. These data confirmed a major activity of BMP/Smad signaling in these cells compared to control ones. As insulin-treatment restored p-Smad1 diabetic profile to control levels, these observations suggest that diabetes positively modulates BMP signaling leading to increased Smad activity in the muscle layer.

A mechanistic explanation for the increased p-Smad1 in diabetic ganglion cells was provided by the observation that BMPR-Ia receptor was upregulated on neurons with a significantly altered expression profile of BMP ligands in the tissue.

We detected BMP-2 as the major ligand in the enteric system involved in BMP activity. Recently it has been shown that BMP-2 promotes the survival of TH-expressing enteric neurons in embryonic cell cultures. Moreover, the differentiation of these nitrergic and catecholaminergic enteric neurons runs through a Smad1-dependent pathway (Anitha et al., 2010). These findings led us to believe that BMP-2 could play a role in the organization of the myenteric plexus, maintaining neuron number in normal conditions. Our results demonstrated that the diabetic state caused a significant decrease in BMP-2 (more evident at 9 weeks) which was correlated with an increased neuronal loss. These results support the importance of BMP-2 in myenteric plexus.

Additionally, in our experimental conditions, no evidence of BMP-4 expression in normal muscle layer was found. In sharp contrast, diabetes in D3w animals caused an ectopical BMP-4 expression in the myenteric ganglia and in the outer muscle layer. It is known that BMP-4 transduces its signal by binding to a heterodimer consisting of a type I receptor (BMPR-Ia) and a type II (BMPR-II) receptor (Nohe et al., 2002). BMP-4 expression accompanied by simultaneous increment in BMPR-Ia receptor could lead to impairment of the cellular mechanisms in the enteric neurons with possible changes in the apoptotic processes.

BMP-2 and BMP-4 have been implicated in the differentiation and survival of enteric neurons during organogenesis (de Santa Barbara et al., 2005; Goldstein et al., 2005; Fu et al., 2006; Faure et al., 2007). It has been shown that BMP-4 has a dual role, promoting or blocking the apoptotic process during the early stages of embryonic development and organogenesis (Bastida et al., 2004; Glavic et al., 2004). In vitro studies evidenced that high concentrations of BMP-4 cause cell death by apoptosis in neuronal precursor cells (Chalazonitis et al., 2004; Gambaro et al., 2006; Chalazonitis et al., 2008). In line with these findings, we suggest that BMP-4 ectopic expression could be involved in apoptotic events of the enteric nervous system. Furthermore, it has been shown that BMP-2 has concentration-dependent effects on enteric neural crest cells in vitro (Pisano et al., 2000; Chalazonitis et al., 2004). In this way, as we suggest above, decreased BMP-2 expression during diabetes could have an additional effect on the survival of myenteric neurons. However, we do not exclude the possibility that other signaling pathways may also be involved in the alterations of the enteric nervous system during early diabetes. In this regard, in vitro and in vivo studies developed in 8 week diabetic mice revealed apoptosis of rodent enteric neurons associated with impaired PI3K/Akt activity (Anitha et al., 2006; Du et al., 2009). This fact could explain the apoptotic effect observed in our D9w animals.

It is interesting to note that treatment of diabetic animals with insulin for 3 weeks prevented changes in BMP-2, BMP-4 and BMPRI expression, maintaining p-Smad levels in D + Ins rats similar to control values. These facts strengthen the argument that altered BMP/Smad signaling would be associated with the diabetic state.

On the hole, our results show that diabetes is accompanied by changes in BMP/Smad signaling in the myenteric plexus of the small

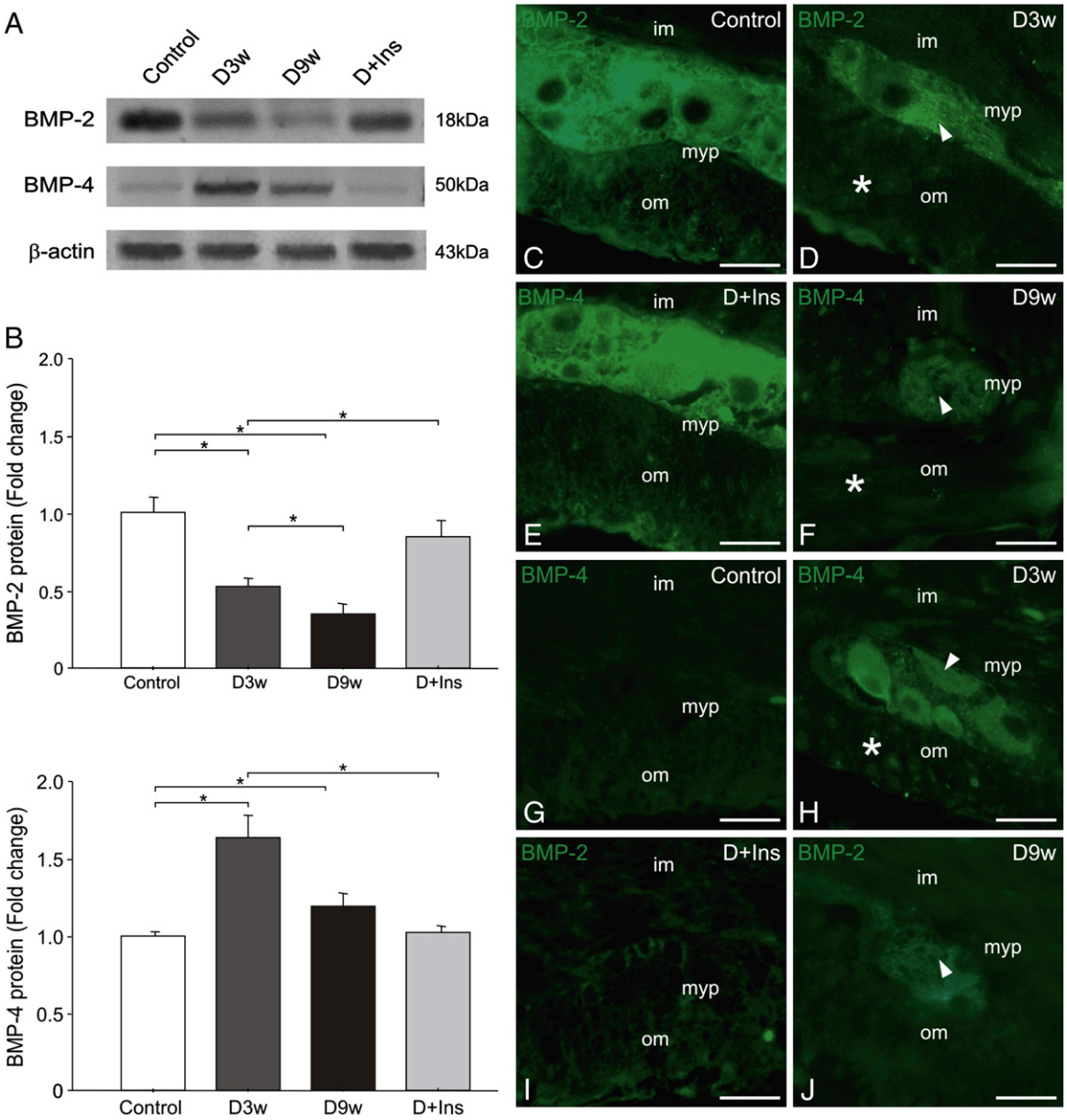

Fig. 7. Relative mean protein levels of BMP-2 and BMP-4 in the jejunal muscle layer of control, D3w, D9w and D + Ins rats are shown in representative Western blot bands (A). A total of 3 independent experiments was performed. Data are normalized to control results for each experiment and are represented as mean ± SEM; *pb0.05; $n = 8$ in each group (B). Representative photomicrographs showing BMP-2 and BMP-4 immunofluorescence in the myenteric plexus of control (C, G), D3w (D, H), D9w, (F, J), D + Ins (E, I) rats. Note the decrease in immunoreactivity for BMP-2 in the myenteric ganglia of D3w (D, arrowhead) and D9w (F, arrowhead) jejunum and in the outer muscle layer (D, F asterisks) of both diabetics groups. An ectopic expression of BMP-4 in the myenteric plexus is also seen in D3w and D9w jejunum (H, J arrowhead) and in the outer muscle layer (H asterisks). D + Ins intestine showed the same BMP-2 BMP-4 expression patterns of control jejunum A total of 3 independent experiments per marker was performed; n = 12 in each group per marker. im: inner muscle layer; myp: myenteric plexus; om: outer muscle layer. Bars: C-J: 20 μm.

intestine. However, the exact mechanism of this change in diabetes is not yet known, and the downstream targets involved are not completely understood. Moreover, the expression of BMP signaling in the smooth muscle layer and the changes produced under the diabetic state are interesting and deserve to be studied in order to increase the understanding of the molecular and cellular bases underlying diabetic enteric dysfunction.

Acknowledgments

This work was supported by Grants from Consejo Nacional de Investigaciones Científicas y Técnicas (CONICET) and Secretaría de Ciencia y Tecnología, Universidad Nacional de Tucumán (CIUNT) to S.S.S. We thank Dr. K. Masuhara (Osaka, JP) for the donation of anti-BMP4. The authors also thank R. Fernandez for his excellent assistance with confocal microscopy and image analysis and Ms. Virginia Méndez for her proofreading. S.M.H. is a recipient of a CONICET (Argentina) Fellowship. S.S.S. is a Career Investigator of CONICET (Argentina).

Appendix A. Supplementary data

Supplementary data to this article can be found online at doi:10.1016/j.autneu.2011.06.003.

References

Aizenman, Y., de Vellis, J., 1987. Synergistic action of thyroid hormone, insulin and hydrocortisone on astrocyte differentiation. Brain Res. 414, 301–308.
Anitha, M., Gondha, C., Sutliff, R., Parsadanian, A., Mwangi, S., Sitaraman, S.V., Srinivasan, S., 2006. GDNF rescues hyperglycemia-induced diabetic enteric neuropathy through activation of the PI3K/Akt pathway. J. Clin. Invest. 116, 344–356.

Anitha, M., Shahnavaz, N., Qayed, E., Joseph, I., Gossrau, G., Mwangi, S., Sitaraman, S.V., Greene, J.G., Srinivasan, S., 2010. BMP2 promotes differentiation of nitrergic and catecholaminergic enteric neurons through a Smad1-dependent pathway. Am J. Physiol. Gastrointest Liver Physiol. 298 (3), G375–G383.
Bastida, M.F., Delgado, M.D., Wang, B., Fallon, J.F., Fernandez-Teran, M., Ros, M.A., 2004. Levels of Gli3 repressor correlate with Bmp4 expression and apoptosis during limb development. Dev. Dyn. 231 (1), 148–160.
Batts, L.E., Polk, D.B., Dubois, R.N., Kulessa, H., 2006. BMP signaling is required for intestinal growth and morphogenesis. Dev. Dyn. 235 (6), 1563–1570.
Baurand, A., Zelarayan, L., Betney, R., Gehrke, C., Dunger, S., Noack, C., Busjahn, A., Huelsken, J., Taketo, M.M., Birchmeier, W., Dietz, R., Bergmann, M.W., 2007. Beta-catenin downregulation is required for adaptive cardiac remodeling. Circ. Res. 100 (9), 1353–1362.
Biolo, G., Stulle, M., Bianco, F., Mengozzi, G., Barazzoni, R., Vasile, A., Panzetta, G., Guarnieri, G., 2008. Insulin action on glucose and protein metabolism during l-carnitine supplementation in maintenance haemodialysis patients. Nephrol. Dial. Transplant. 23, 991–997.
Brewer, K.C., Mwizerva, O., Goldstein, A.M., 2005. BMPRIA is a promising marker for evaluating ganglion cells in the enteric nervous system–a pilot study. Hum. Pathol. 36 (10), 1120–1126.
Büttow, N.C., Miranda Neto, M.H., Bazotte, R.B., 1997. Morphological and quantitative study of the myenteric plexus of the duodenum of streptozotocin-induced diabetic rats. Arq. Gastroenterol. 34 (1), 34–42.
Bytzer, P., Talley, N.J., Leemon Young, L.J., Jones, M.P., Horowitz, M., 2001. Prevalence of gastrointestinal symptoms associated with diabetes mellitus: a population-based survey of 15,000 adults. Arch. Intern. Med. 161, 1989–1996.
Bywater, R.A., Taylor, G.S., Furukawa, K., 1987. The enteric nervous system in the control of motility and secretion. Dig. Dis. 5 (4), 193–211.
Caldeira, E., Cagnon, V., 2008. IGF-I and INS receptor expression in the salivary glands of diabetic Nod mice submitted to long-term insulin treatment. Cell Biol Int. 32 (1), 16–21.
Camilleri, M., Malagelada, J.R., 1984. Abnormal intestinal motility in diabetics with the gastroparesis syndrome. Eur. J. Clin. Invest. 14 (6), 420–427.
Chalazonitis, A., D'Autreaux, F., Guha, U., Pham, T.D., Faure, C., Chen, J.J., et al., 2004. Bone morphogenetic protein-2 and -4 limit the number of enteric neurons but promote development of a TrkC-expressing neurotrophin- 3-dependent subset. J. Neurosci. 24, 4266–4282.
Chalazonitis, A., Pham, T.D., Li, Z., Roman, D., Guha, U., Gomes, W., Kan, L., Kessler, J.A., Gershon, M.D., 2008. Bone morphogenetic protein regulation of enteric neuronal phenotypic diversity: relationship to timing of cell cycle exit. J. Comp. Neurol. 509 (5), 474–492.
Chandrasekharan, B., Srinivasan, S., 2007. Diabetes and the enteric nervous system. Neurogastroenterol. Motil. 19, 951–960.
Chandrasekharan, B., Anitha, M., Blatt, R., Shahnavaz, N., Kooby, D., Staley, C., Mwangi, S., Jones, D.P., Sitaraman, S.V., Srinivasan, S., 2011. Colonic motor dysfunction in human diabetes is associated with enteric neuronal loss and increased oxidative stress. Neurogastroenterol. Motil. 23 (2), 131–138, e26.
Coleman, E., Dennis, J., Braden, T., Judd, R., Posner, P., 2010. Insulin treatment prevents diabetes-induced alterations in astrocyte glutamate uptake and GFAP content in rats at 4 and 8 weeks of diabetes duration. Brain Res. 1306, 131–141.
de Santa Barbara, P., Williams, J., Goldstein, A.M., Doyle, A.M., Nielsen, C., Winfield, S., Faure, S., Roberts, D.J., 2005. BMP signaling pathway plays multiple roles during gastrointestinal tract development. Dev. Dyn. 234, 312–322.
Du, F., Wang, L., Qian, W., Liu, S., 2009. Loss of enteric neurons accompanied by decreased expression of GDNF and PI3K/Akt pathway in diabetic rats. Neurogastroenterol. Motil. 21 (11), 1229-e114.
Faure, C., Chalazonitis, A., Rhéaume, C., Bouchard, G., Sampathkumar, S.G., Yarema, K.J., Gershon, M.D., 2007. Gangliogenesis in the enteric nervous system: roles of the polysialylation of the neural cell adhesion molecule and its regulation by bone morphogenetic protein-4. Dev. Dyn. 236 (1), 44–59.
Feng, X.H., Derynck, R., 2005. Specificity and versatility in TGF-beta signaling through Smads. Annu. Rev. Cell. Dev. Biol. 21, 659–693.
Fregonesi, C.E., Miranda-Neto, M.H., Molinari, S.L., Zanoni, J.N., 2001. Quantitative study of the myenteric plexus of the stomach of rats with streptozotocin-induced diabetes. Arq. Neuropsiquiatr. 59 (1), 50–53.
Fu, M., Vohra, B.P., Wind, D., Heuckeroth, R.O., 2006. BMP signaling regulates murine enteric nervous system precursor migration, neurite fasciculation, and patterning via altered Ncam1 polysialic acid addition. Dev. Biol. 299 (1), 137–150.
Furlan, M.M., Molinari, S.L., Miranda Neto, M.H., 2002. Morphoquantitative effects of acute diabetes on the myenteric neurons of the proximal colon of adult rats. Arq. Neuropsiquiatr. 60, 576–581.
Gambaro, K., Aberdam, E., Virolle, T., Aberdam, D., Rouleau, M., 2006. BMP-4 induces a Smad-dependent apoptotic cell death of mouse embryonic stem cell-derived neural precursors. Cell Death Differ. 13 (7), 1075–1087.
Glavic, A., Honoré, S.M., Gloria, Feijóo C., Bastidas, F., Allende, M.L., Mayor, R., 2004. Role of BMP signaling and the homeoprotein Iroquois in the specification of the cranial placodal field. Dev. Biol. 272 (1), 89–103.
Goldstein, A.M., Brewer, K.C., Doyle, A.M., Nagy, N., Roberts, D.J., 2005. BMP signaling is necessary for neural crest cell migration and ganglion formation in the enteric nervous system. Mech. Dev. 122 (6), 821–833.
Goyal, R.K., Spiro, H.M., 1971. Gastrointestinal manifestations of diabetes mellitus. Med. Clin. North Am. 55, 1031–1044.
Grunz, H., 1996. Factors responsible for the establishment of the body plan in the amphibian embryo. Int. J. Dev. Biol. 40 (1), 279–289.
He, C.L., 2001. Loss of interstitial cells of cajal and inhibitory innervation in insulindependent diabetes. Gastroenterology 121, 427–434.
Hernandes, L., Bazotte, R.B., Gama, P., Miranda-Neto, M.H., 2000. Streptozotocin-induced diabetes duration is important to determine changes in the number and basophily of myenteric neurons. Arq. Neuropsiquiatr. 58 (4), 1035–1039.
Horowitz, M., Maddox, A.F., Wishart, J.M., Harding, P.E., Chatterton, B.E., Shearman, D.J., 1991. Relationships between oesophageal transit and solid and liquid gastric emptying in diabetes mellitus. Eur J Nucl Med 18 (4), 229–234.
Huang, T., Price, S., Chilton, L., Calcutt, N., Tomlinson, D., Verkhratsky, A., Fernyhough, P., 2003. Insulin prevents depolarization of the mitochondrial inner membrane in sensory neurons of type 1 diabetic rats in the presence of sustained hyperglycemia. Diabetes 52, 2129–2136.
Jabbur, S.J., el-Kak, F.H., Nassar, C.F., 1988. The enteric nervous system—an overview. Med. Res. Rev. 8 (3), 459–469.
Kniel, P., Junker, U., Perrin, I.V., Bestetti, G.E., Rossi, G.L., 1996. Varied effects of experimental diabetes on the autonomic nervous system of the rat. Lab. Invest. 54, 523–530.
Koch, K.L., 1999. Diabetic gastropathy: gastric neuromuscular dysfunction in diabetes mellitus: a review of symptoms, pathophysiology, and treatment. Dig. Dis. Sci. 44 (6), 1061–1075.
Lee, P.G., Hohman, T.C., Cai, F., Regalia, J., Helke, C.J., 2001. Streptozotocin-induced diabetes causes metabolic changes and alterations in neurotrophin content and retrograde transport in the cervical vagus nerve. Exp. Neurol. 170, 149–161.
Lee, P.G., Cai, F., Helke, C.J., 2002. Streptozotocin-induced diabetes reduces retrograde axonal transport in the afferent and efferent vagus nerve. Brain 941, 127–136.
Liu, W., Yue, W., Wu, R., 2010. Effects of diabetes on expression of glial fibrillary acidic protein and neurotrophins in rat colon. Autonomic Neuroscience: Basic and Clinical 154, 79–83.
Lowry, O.H., Rosenbrough, J., Farr, A.L., Randall, R.J., 1951. Protein measurement with the Folin phenol reagent. J. Biol. Chem. 193, 265–275.
Nakabou, Y., Okita, C., Takano, Y., Hagihira, H., 1974. Hyperplastic and hypertrophic changes of the small intestine in alloxan diabetic rats. J. Nutr. Sci. Vitaminol. (Tokyo) 20 (3), 227–234.
Nohe, A., Hassel, S., Ehrlich, M., Neubauer, F., Sebald, W., Henis, Y.I., Knaus, P., 2002. The mode of bone morphogenetic protein (BMP) receptor oligomerization determines different BMP-2 signaling pathways. J. Biol. Chem. 277 (7), 5330–5338.
Pisano, J.M., Colon-Hastings, F., Birren, S.J., 2000. Postmigratory enteric and sympathetic neural precursors share common, developmentally regulated, responses to BMP2. Dev. Biol. 227, 1–11.
Rayner, C.K., Horowitz, M., 2006. Gastrointestinal motility and glycemic control in diabetes: the chicken and the egg revisited? J. Clin. Invest. 116 (2), 299–302.
Rayner, C.K., Samsom, M., Jones, K.L., Horowitz, M., 2001. Relationships of upper gastrointestinal motor and sensory function with glycemic control. Diabetes Care. 24, 371–381.
Ricci, J.A., Siddique, R., Stewart, W.F., Sandler, R.S., Sloan, S., Farup, C.E., 2000. Upper gastrointestinal symptoms in a U.S. national sample of adults with diabetes. Scand. J. Gastroenterol. 35 (2), 152–159.
Rosendahl, A., Pardali, E., Speletas, M., ten Dijke, P., Heldin, C., Sideras, P., 2002. Activation of bone morphogenetic protein/Smad signaling in bronchial epithelial cells during airway inflammation. Am. J. Respir. Cell Mol. Biol. 27, 160–169.
Rubin, D.C., 2007. Intestinal morphogenesis. Curr. Opin. Gastroenterol. 23 (2), 111–114.
Rühl, A., 2005. Glial cells in the gut. Neurogastroenterol. Motil. 17, 777–790.
Rühl, A., Nasser, Y., Sharkey, K.A., 2004. Enteric glia. Neurogastroenterol. Motil. 16 (Suppl 1), 44–49.
Sánchez, S.S., Genta, S.B., Aybar, M.J., Honoré, S.M., Villecco, E.I., Sánchez Riera, A.N., 2000. Changes in the expression of small intestine extracellular matrix proteins in streptozotocin-induced diabetic rats. Cell. Bio.l Int. 24 (12), 881–888.
Schmeichel, A.M., Schmelzer, J.D., Low, P.A., 2003. Oxidative injury and apoptosis of dorsal root ganglion neurons in chronic experimental diabetic neuropathy. Diabetes 52, 165–171.
Shi, Y., Massagué, J., 2003. Mechanisms of TGF-beta signaling from cell membrane to the nucleus. Cell 113 (6), 685–700.
Spångéus, A., El-Salhy, M., Suhr, O., Eriksson, J., Lithner, F., 1999. Prevalence of gastrointestinal symptoms in young and middle-aged diabetic patients. Scand. J. Gastroenterol. 34 (12), 1196–1202 Dec.
Toran-Allerand, C.D., Bentham, W., Miranda, R.C., Anderson, J.P., 1991. Insulin influences astroglial morphology and glial fibrillary acidic protein (GFAP) expression in organotypic cultures. Brain Res. 558, 296–304.
Tougas, G., Hunt, R.H., Fitzpatrick, D., Upton, A.R., 1992. Evidence of impaired afferent vagal function in patients with diabetes gastroparesis. Pacing Clin. Electrophysiol. 15, 1597–1602.
Unger, J.W., Klitzsch, T., Pera, S., Reiter, R., 1998. Nerve growth factor (NGF) and diabetic neuropathy in the rat: morphological investigations of sural nerve, dorsal root ganglion and spinal cord. Exp. Neurol. 153, 23–34.
Wang, C., Li, Y., Wible, B., Angelides, K., Ishii, D., 1992. Effects of insulin and insulin-like growth factors on neurofilament mRNA and tubulin mRNA content in human neuroblastoma SH-SY5Y cells. Brain Res Mol Brain Res 13, 289–300.
Watkins, C.C., Sawa, A., Jaffrey, S., Blackshaw, S., Barrow, R.K., Snyder, S.H., Ferris, C.D., 2000. Insulin restores neuronal nitric oxide synthase expression and function that is lost in diabetic gastropathy. J. Clin. Invest. 106, 373–384.
Yoneda, S., Kadowaki, M., Kuramoto, H., Fukui, H., Takaki, M., 2001. Enhanced colonic peristalsis by impairment of nitrergic enteric neurons in spontaneously diabetic rats. Auton. Neurosci. 92, 65–71.
Zador, I., Deshmukh, G., Kunkel, R., Johnson, K., Radin, N., Shayman, J., 1993. A role for glycosphingolipid accumulation in the renal hypertrophy of streptozotocin-induced diabetes mellitus. Clin Invest. 91 (3), 797–803.
Zwijsen, A., Verschueren, K., Huylebroeck, D., 2003. New intracellular components of bone morphogenetic protein/Smad signaling cascades. FEBS Lett. 546 (1), 133–139.